

Pseudo-Stereo Inputs: A Solution to the Occlusion Challenge in Self-Supervised Stereo Matching

Ruizhi Yang, Xingqiang Li, Jiajun Bai, Jinsong Du

Abstract—Self-supervised stereo matching holds great promise for application and research due to its independence from expensive labeled data. However, direct self-supervised stereo matching paradigms based on photometric loss functions have consistently struggled with performance issues due to the occlusion challenge. The crux of the occlusion challenge lies in the fact that the positions of occluded pixels consistently align with the epipolar search direction defined by the input stereo images, leading to persistent information loss and erroneous feedback at fixed locations during self-supervised training. In this work, we propose a simple yet highly effective pseudo-stereo inputs strategy to address the core occlusion challenge. This strategy decouples the input and feedback images, compelling the network to probabilistically sample information from both sides of the occluding objects. As a result, the persistent lack of information in the aforementioned fixed occlusion areas is mitigated. Building upon this, we further address feedback conflicts and overfitting issues arising from the strategy. By integrating these components, our method achieves stable and significant performance improvements compared to existing methods. Quantitative experiments are conducted to evaluate the performance. Qualitative experiments further demonstrate accurate disparity inference even at occluded regions. These results demonstrate a significant advancement over previous methods in the field of direct self-supervised stereo matching based on photometric loss. The proposed pseudo-stereo inputs strategy, due to its simplicity and effectiveness, has the potential to serve as a new paradigm for direct self-supervised stereo matching. Code is available at <https://github.com/qrzhang/Pseudo-Stereo>.

Index Terms—Stereo matching, self-supervised learning, occlusion challenge

I. INTRODUCTION

Stereo matching, a cost-effective method for obtaining reliable 3D information, has been a longstanding focus of research in computer vision [1]. In recent years, learning-based stereo matching methods have emerged, demonstrating superior performance in terms of accuracy and efficiency [2]–[4]. Nevertheless, the dependence on extensive and often

This work was supported in part by the National Natural Science Foundation of China under Grant 62101547. (Corresponding authors: Xingqiang Li; Jinsong Du.)

Ruizhi Yang is with the Shenyang Institute of Automation, Chinese Academy of Sciences, Shenyang 110016, China, also with the Liaoning Liaohe Laboratory, Shenyang 110169, China, also with the Key Laboratory on Intelligent Detection and Equipment Technology of Liaoning Province, Shenyang 110169, China, and also with the University of Chinese Academy of Sciences, Beijing 100049, China (e-mail: yangruizhi@sia.cn).

Xingqiang Li, Jiajun Bai, and Jinsong Du are with the Shenyang Institute of Automation, Chinese Academy of Sciences, Shenyang 110016, China, also with the Liaoning Liaohe Laboratory, Shenyang 110169, China, and also with the Key Laboratory on Intelligent Detection and Equipment Technology of Liaoning Province, Shenyang 110169, China (e-mail: lixingqiang@sia.cn; baijiajun@sia.cn; jsdu_sia@163.com).

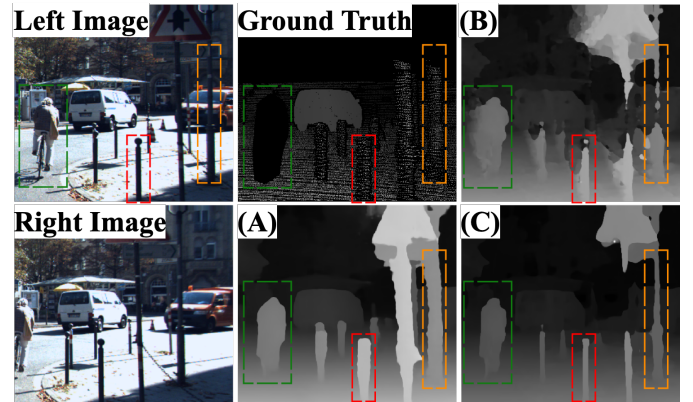


Fig. 1. A comparison of various training methods in stereo matching, including a supervised method (A), the existing self-supervised paradigm (B), and our proposed self-supervised paradigm (C). (A) underscores the limitation of supervised learning, which relies heavily on accurate ground truth data. (B) illustrates that existing self-supervised methods fail to address the occlusion challenge. Our method (C) demonstrates significantly higher accuracy in the comparison within the marked boxes, showcasing both its independence from ground truth and its ability to solve the occlusion challenge.

difficult-to-acquire annotated datasets for training poses a substantial barrier to wider adoption.

Self-supervised stereo matching methods have emerged as a promising approach to address this challenge, attracting growing interest and research efforts. By exploiting the principle of photometric consistency across different viewpoints for network training [5]–[8], this method eliminates the need for ground truth data. This crucial attribute notably improves the practicality and extends the scope of application for learning-based stereo matching methods. However, the photometric consistency assumption is not always valid. Typically, in occluded regions where there are no corresponding pixels from another viewpoint, the network tends to predict disparities that point towards the most similar pixels. This results in noticeable errors in disparity prediction. There has been substantial effort dedicated to addressing this issue. For example, [6] attempted to incorporate the left-right consistency assumption into the loss function, penalizing discrepancies in left and right disparity predictions. [8] discarded the losses corresponding to pixels with inconsistent left-right disparity during training, which is also a common strategy used in self-supervised optical flow estimation tasks facing similar challenges [9], [10]. Nevertheless, despite these efforts, errors in predicting occluded regions persist and notably limit the accuracy of their predictions. The main cause of this phenomenon is the absence of information in occluded regions. Neither left-

right consistency nor smoothness loss can compensate for this missing information. [11] attempted to supplement the missing information by leveraging planar relationships of pixels, observing moderate success. However, their method is overly reliant on the results of edge detection, and forcing non-edge pixels into a planar structure is not consistently accurate. Consequently, existing direct self-supervised stereo matching methods that rely on photometric consistency continue to be significantly hindered by occlusion issues, leading to limited performance.

It is worth noting that self-supervised depth estimation tasks, which also utilize stereo image pairs for feedback, encounter similar challenges. However, as depth estimation only uses a single image as network input, a simple flip augmentation strategy can largely mitigate this problem [12]. Specifically, horizontal flipping can prevent occlusion regions from consistently appearing on a single side of the occluding object. This allows monocular networks to have a certain probability of obtaining information from both sides of the occluding object. However, stereo matching networks require a stereo image pair as input, with the relative position of the left and right images being fixed. This makes it impossible to directly implement this strategy. This limitation was also mentioned and analyzed in detail in [13]. This notably allows self-supervised monocular depth estimation methods to achieve significantly better performance in occluded regions compared to self-supervised stereo matching methods. This observation has led to the development of several methods that leverage depth estimation results to train stereo matching networks. [14] leverages single images and depth maps predicted by depth network to generate a stereo image dataset with disparity labels. [13] trains a monocular completion network using the same training method employed for self-supervised depth estimation. A Consensus mechanism filters and refines the predictions from this network, which then serve as ground truth labels for the supervised training of a stereo matching network. These methods outperform previous direct self-supervised approaches based on the photometric loss. However, they also significantly increase the complexity of training and reliance on monocular depth estimation, which diminishes practical applicability.

This work presents a straightforward strategy to overcome the challenge of consistently lacking information in occluded regions for self-supervised stereo matching. Specifically, we recognize the fundamental difference between stereo and monocular networks in this issue: monocular inputs can leverage feedback images independent of the input itself, while in stereo networks, the relative positions between input and feedback image pairs are fixed. This leads to consistently unchanged locations of missing information in self-supervised stereo matching. Recognizing this fundamental distinction, it becomes clear that the core challenge lies in making the input and feedback images independent for stereo networks. Given that the feedback images must be reliable and thus should not be arbitrarily adjusted, we focus our attention on the input images. Based on this principle, we introduce the pseudo-stereo inputs strategy. This approach substitutes the original inputs with generated inputs that contain a pseudo-image \tilde{I}^R ,

created using the estimated disparity map output by the training network at the current time step. In contrast to methods based on dataset generation [13], [14], our approach does not rely on any previously trained networks. Pseudo-image generation solely relies on the current training network, with image accuracy improving iteratively throughout the training process. Further details are presented and discussed in Section III-A. After sequentially addressing the feedback conflicts and overfitting issues in Section III-B, this method demonstrates a stable and significant performance improvement compared to previous paradigms. By employing this approach, our self-supervised pipeline achieves competitive performance with the earlier representative supervised method DispNetC [2], without utilizing any previously trained models, post-processing techniques, or knowledge distillation strategies. This has significantly advanced the benchmarks for existing direct self-supervised stereo matching methods. In summary, the main contributions of this work are as follows.

- 1) A pseudo-stereo inputs strategy is introduced to address the persistent occlusion challenge that limits self-supervised stereo matching development.
- 2) Several other measures are proposed to further address the feedback conflicts and overfitting problem, resulting in a stable performance improvement.
- 3) This work provides a straightforward implementation that demonstrably improves the performance of direct self-supervised stereo matching methods, establishing it as a new potential paradigm.

II. RELATED WORK

A. Learning-Based Stereo Matching Networks

Deep learning-based stereo matching methods have demonstrated superior accuracy compared to traditional approaches, leading to a surge in research interest in recent years [15]. A diverse range of methods and network architectures with unique capabilities have emerged. For example, DispNetC [2], leveraging correlation layers, boasts high matching speed. PSMNet [3], employing a 4D cost volume, achieves superior accuracy. Recent advancements have further boosted performance through different approaches. Approaches like Los [4], which emphasizes local structure information, and Temporally Consistent Stereo Matching [16], which incorporates temporal consistency, have achieved remarkable results, exhibiting both higher accuracy and faster processing speeds. Among the aforementioned methods, PSMNet, a well-established and widely-used network architecture, is frequently employed as a base network for self-supervised methods to validate their effectiveness [13], [14], [17]. Therefore, we also adopt PSMNet as our backbone in this study to facilitate comparisons.

B. Self-Supervised Stereo Matching

1) *Direct Methods based on Photometric Loss:* Direct methods based on photometric loss have been widely adopted in self-supervised stereo matching [5], [7], [8], [11], [18], self-supervised depth estimation [12], [19]–[21], and self-supervised optical flow estimation [9], [10], [22]. These approaches rely on the principle that images captured from

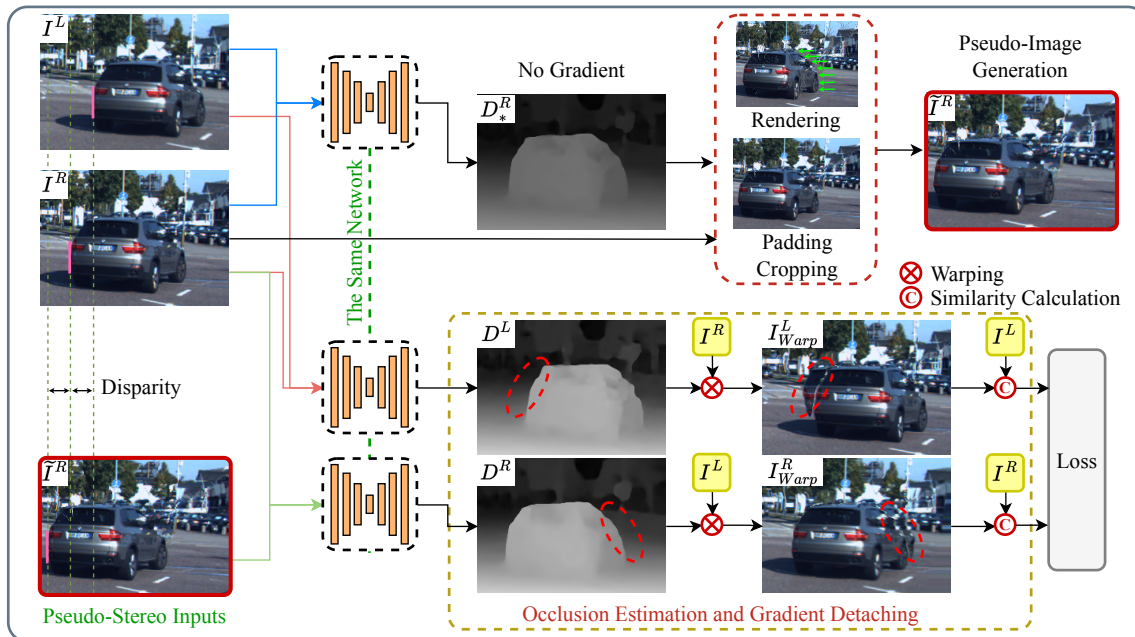


Fig. 2. Overview of the pseudo-stereo inputs strategy. The core elements encompass the pseudo-image generation method, the pseudo-stereo inputs training strategy using pseudo-images, along with the occlusion estimation and gradient detaching that aimed at resolving feedback conflicts, as well as additional methods for addressing overfitting issues (not illustrated here).

different viewpoints should exhibit consistent brightness and color. By warping images from secondary viewpoints to align with the primary viewpoint, the methods calculate losses based on discrepancies in both photometric properties and structural details. Nevertheless, such approaches have consistently suffered from precision limitations due to factors like occlusion, which violate the assumptions of photometric consistency. In self-supervised stereo matching, various methods have been attempted to address this issue. Typical approaches include estimating and blocking the propagation of loss at occluded positions [8], penalizing inconsistencies between left and right disparity predictions [6], and exploiting adjacent information within a single image to infer disparities in occluded regions [11]. Despite these efforts, their matching performance remains constrained by occlusion problems and struggles to improve significantly.

2) *Methods based on Dataset Generation*: Training networks on synthetic datasets, which are readily available with labels, is a common practice [2]. However, due to the discrepancies between synthetic and real-world datasets, models often struggle to achieve high performance when deployed in real-world scenarios. Consequently, methods based on dataset generation have emerged that aim to generate labeled datasets from real images. [14] employs a previously trained depth estimation model to generate depth maps from single images. By combining these depth maps with the original images, they create synthetic stereo pairs and corresponding disparity labels. [13] trained a monocular completion network using the self-supervised training methods based on photometric loss. This network takes sparse disparity maps obtained through traditional methods and the original images as input, outputting dense disparity maps. The trained network can then be used

to generate labeled datasets. The generated disparity maps are further refined using a consensus mechanism to remove unreliable disparity values and this distillation process significantly improves the quality of the labels, leading to superior performance for networks trained using the generated datasets. Additionally, [17] also achieved good matching accuracy by generating datasets using NeRF (Neural Radiance Fields). However, as NeRF requires numerous images of a specific scene with camera pose information as inputs, this method cannot be directly applied to common datasets like KITTI, unlike the methods previously discussed.

Overall, in self-supervised stereo matching, methods based on dataset generation have significantly outperformed direct methods based on photometric loss. The pseudo-stereo inputs strategy proposed in this paper changes this landscape. By applying this strategy, we can achieve competitive performance with a substantially lower training complexity compared to dataset generation-based approaches.

III. METHOD

The overall framework of our method is illustrated in Figure 2. Section III-A details the core idea in our approach: a pseudo-stereo inputs strategy that decouples input images from feedback images. Section III-B further discusses the additional challenges encountered during implementation and proposes solutions, including addressing feedback conflicts and overfitting problems. The final loss functions are also presented in this section.

A. Pseudo-Stereo Inputs Strategy

This section elucidates the principles and implementation of our pseudo-stereo inputs strategy, which addresses the

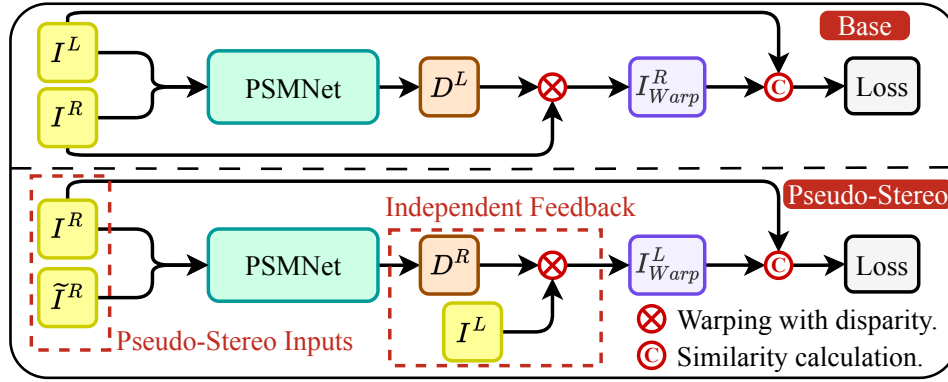


Fig. 3. A comparison between the existing self-supervised pipeline and our pseudo-stereo inputs strategy. In contrast to existing methods, our method decouples the input stereo images from the feedback stereo images. This allows for flexible feedback using image pairs with different occlusion positions.

occlusion challenge by decoupling the input image pairs from the feedback image pairs in self-supervised training. The core method for this decoupling is to utilize image pairs containing a generated pseudo-image as inputs instead of original image pairs. In contrast, the feedback calculation relies solely on the original images to ensure the reliability and accuracy of the feedback. This decoupling removes the fixed relative positional constraints on the input and feedback images, allowing them to flexibly select positions where occlusions occur, thereby addressing the issue of continuous information loss due to fixed occlusions. The following subsections provide a detailed discussion.

1) *Pseudo-Stereo Inputs*: Figure 3 visually illustrates the distinction between this strategy and existing self-supervised paradigms. In this strategy, the left view remains a real image from the dataset, while the right view is replaced with a generated pseudo-image. Specifically, existing methods use a stereo image pair I^L, I^R from the dataset as network inputs and output a disparity map D^L aligned with I^L . Where I and D denote color images and disparity maps, respectively. Superscripts L and R indicate correspondence to the original left and right viewpoints. In contrast, when using pseudo-inputs, an estimated disparity D^R and I^R are used to generate a pseudo-image \tilde{I}^R . At this point, the network inputs become I^R as the left view and \tilde{I}^R as the right view, producing a dense disparity map D^R aligned with I^R . As mentioned previously, the images used for feedback should be the original ones to ensure reliability. Therefore, the original image I^L is warped using D^R to obtain I^L_{Warp} , which is aligned with I^R . I^R and I^L_{Warp} are then employed for loss calculation. When I^L is as the left input, the occluded areas appear to the left of the occluders; conversely, when I^R is as the left input, the occluded areas are on the right side of the occluders. This strategy ensures that the network can consistently have a probability to capture information from both sides of the occluders, thus resolving the problem where previous methods invariably lacked information from one side of the occluders.

2) *Discussion on Using Pseudo-Stereo Images as Inputs*: Our method differs from data generation-based methods [13], [14], [17] which use a previously trained network to generate data. Instead, the generation of pseudo-images relies on the

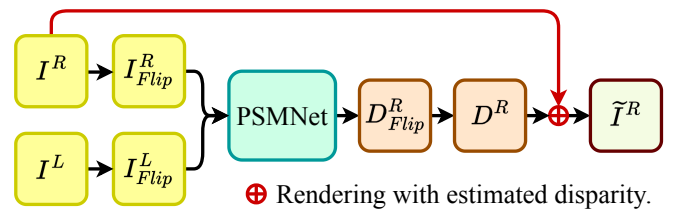


Fig. 4. Schematic diagram of the pseudo-images generation using the rendering method, where PSMNet is the model currently under training rather than a previously well-trained one. The subscript “Flip” denotes horizontal flipping.

network that is currently undergoing training and occurs throughout the entire training process. In other words, images generated in the early stages of training, which severely lack realism, are also used as inputs during the training process. This raises concerns about the network’s convergence. However, in fact, it is desirable during stereo matching network training to force the network not to overly rely on binocular information and instead seek clues within a single image. As an example, in the supervised training method [23], random patches are used to occlude the right view to accomplish this objective. Our strategy encourages the network to leverage monocular cues in the initial stages of training to enhance prediction accuracy. As accuracy increases, the precision of pseudo-image generation also improves, leading to better binocular information for the network. This results in a stable and progressively enhancing iterative process. The experimental results in Section IV-B also support this point. In these experiments, even when no real images were used for the right input (i.e., using I^L, \tilde{I}^L or I^R, \tilde{I}^R as network inputs), the network still converges successfully. This outcome is consistent with our expectations.

3) *Method for Generating Pseudo-Images*: While the most common warping operation in stereo matching involves using D^L , which is aligned with I^L , to warp I^R into an image that aligns with I^L , this approach cannot be used for generating pseudo-images. The reason is that we do not have a disparity map aligned with the pseudo-image prior to its generation. Consequently, our approach employs a pseudo-image generation method that more closely resembles a simplified rendering

process as illustrated in Figure 4. For I^R , each pixel can be relocated backward using D^R to generate \tilde{I}^R . If multiple pixels map to the same location in \tilde{I}^R , only the pixel with the maximum disparity is kept. This corresponds to the occlusion effect during rendering. As shown in Figure 5, this process yields a pseudo-image containing missing pixels. To make it as similar to the real image as possible, it is necessary to pad these missing pixels. The padding method and how closely the resulting image resembles a real one directly influence the severity of the overfitting problem. This issue is discussed in detail in Section III-B.

B. Feedback Conflicts and Overfitting Problems

Simply applying the pseudo-stereo inputs strategy with no further modifications already results in network performance that far surpasses current direct self-supervised methods, which can be evident from the ablation experiments in Section IV-B. Nevertheless, there remains a considerable gap when compared to dataset generation-based methods [13]. Our further experiments observed that feedback conflicts and overfitting problems are the reasons hindering further performance improvements. Specifically, as training progresses, the prediction in occluded regions becomes unstable, and the matching accuracy shows a declining trend towards the later stages of training.

1) *Feedback Conflicts*: This phenomenon can be readily explained. Despite our strategy in self-supervised feedback ensuring a 50% probability of obtaining correct information on the occluded side, there remains an equal 50% probability of receiving incorrect information. Although the information is always conflicting, it is expected that the network will attempt to minimize the loss of both correct and incorrect information simultaneously, resulting in a compromised outcome in the occluded region. As the gradient of photometric loss is negatively correlated with image similarity, correct disparity estimations receive lower gradients due to high similarity in later training stages. Conversely, incorrect estimations obtain higher gradients due to low similarity, thus dominating the optimization process. This phenomenon contributes to the instability observed in the occluded region.

Occlusion estimation and detaching the propagation of loss from occluded pixels offers a promising solution to this challenge. While consistency check [24] and backward warping [25] are prevalent methods for occlusion estimation, they necessitate estimating the disparity map from the other viewpoint. This dependency makes the unreliability of the other view’s disparity prediction severely detrimental to the accuracy of occlusion estimation. We implement a solution based on the rendering method described in Section III-A3 for direct occlusion estimation. Specifically, we identify invalid pixels during the rendering process – those falling outside the image boundaries or occluded by other pixels – and classify them as occlusion pixels. This method leverages the inherent properties of the current view rather than relying on information from another view to determine pixel validity. Consequently, it effectively minimizes the risk of misclassifying non-occlusion pixels and prevents erroneous feedback from propagating.

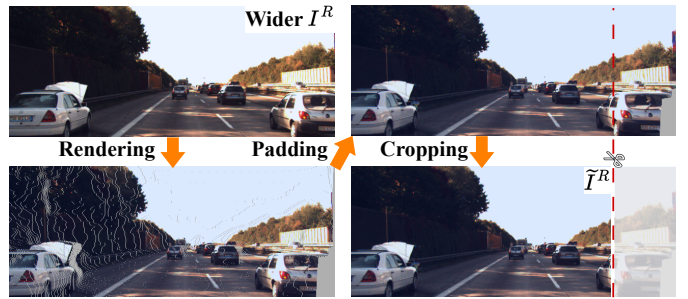


Fig. 5. Visual demonstration of the pseudo-image generation process. Issues with small-scale pixel loss and large-scale pixel missing at edges are mitigated using padding and cropping.

After mitigating erroneous feedback stemming from occluded pixels using this approach, we observe a notable improvement in the network’s performance. Detailed results can be found in the ablation study presented in Section IV-B. Subsequently, the photometric loss L_p can be expressed as:

$$L_p = \frac{1}{N} \sum_{ij} (p \cdot pe(I_{ij}^L, I_{ij}^R) + (1-p) \cdot pe(I_{ij}^R, \tilde{I}_{ij}^R)) \cdot \tilde{O}_{ij} \quad (1)$$

$$\text{where } pe(I^A, I^B) = \frac{\alpha}{2} (1 - SSIM(I^A, I^B)) + (1 - \alpha) \|I^A - I^B\|_1 \quad (2)$$

Here, p and $1-p$ represent the probabilities of the respective items, both being constant at 0.5. \tilde{O}_{ij} denotes the occlusion estimation value, where it equals 1 for non-occluded pixels and 0 for occluded ones. $\alpha = 0.85$ as in [12].

2) *Overfitting Problems*: Incorporating occlusion estimation into the pseudo-stereo inputs strategy further enhances performance. Nevertheless, extended long-term training stability tests have revealed the overfitting problem. Further analysis of the experimental images reveals that this issue stems from the network’s ability to distinguish between real and pseudo images in the later stages of training. Specifically, in current strategies, the use of real or pseudo image pairs directly determines the location of occlusions. This enables the network to classify inputs by detecting whether they are pseudo images, thereby converging different results for each input type. This renders the network no longer “consistently have a probability to capture information from both sides of the occluders” as expected. These observations suggest that the generated pseudo-images contain sufficient features for the network to distinguish them. Based on this inference, we initially attempted to generate more indistinguishable images to prevent the network from classifying the inputs. When generating images using the rendering method described in Section III-A3, notable features include small-scale voids at occluded areas and large-scale missing areas along the right edge, as shown in Figure 5. For small-scale voids, we fill them using the average value of adjacent non-void pixels. For the missing parts at the right edge, we adopt a wider generation strategy to produce images that are wider than the inputs. This ensures that the resulting cropped images no longer suffer from large-scale missing regions at their edges. It is evident that

TABLE I

COMPARISON WITH EXISTING METHODS ON THE KITTI ONLINE BENCHMARK, INCLUDING REPRESENTATIVE SUPERVISED METHODS (S), SELF-SUPERVISED METHODS BASED ON DATASET GENERATION (D), AND DIRECT SELF-SUPERVISED METHODS BASED ON PHOTOMETRIC CONSISTENCY (P). THE BEST RESULTS IN EACH CATEGORY ARE HIGHLIGHTED IN BOLD.

Method		KITTI 2012 Test				KITTI 2015 Test			
		3-noc (%)	3-all (%)	EPE-noc	EPE-all	D1-bg (%)	D1-fg (%)	D1-all (%)	D1-noc (%)
<i>Supervised methods - Training with ground truth</i>									
S	DispNetC [2]	4.11	4.65	0.9	1.0	4.32	4.41	4.34	4.05
	PSMNet [3]	1.49	1.89	0.5	0.6	1.86	4.62	2.32	2.14
	LoS [4]	1.10	1.38	0.4	0.4	1.42	2.81	1.65	1.52
<i>Self-supervised methods - Based on dataset generation</i>									
D	MfS-PSMNet [14]	-	[4.43]	-	[0.95]	-	-	[4.75]	[4.57]
	NS-PSMNet [17]	-	-	-	-	-	-	[5.05]	[4.80]
	Rversing-PSMNet [13]	-	-	-	-	3.13	8.7	4.06	3.86
<i>Direct self-supervised methods - Based on photometric consistency</i>									
P	OASM [6]	6.39	8.60	1.3	2.0	6.89	19.42	8.98	7.39
	PASMnet [8]	-	-	-	-	5.41	16.36	7.23	6.69
	UHP [11]	6.05	7.09	1.2	1.3	5.00	13.7	6.45	5.93
	Flow2Stereo [22]	4.58	5.11	1.0	1.1	5.01	14.62	6.61	6.29
	CRD-Fusion [26]	4.38	5.40	0.9	1.1	4.59	13.68	6.11	5.69
	Pseudo-Stereo (ours)	3.46	4.08	0.8	0.9	3.11	12.52	4.68	4.40

the generated images now possess a higher degree of realism. Under this strategy, experiments demonstrate an improvement in overfitting issues; however, they have not been completely eradicated. This implies that the network is still able to extract subtle features for differentiation.

We further implement the fully pseudo-stereo inputs strategy. This strategy no longer relies on real image pairs but instead uses fully pseudo-stereo images as input. To be specific, the network’s inputs are changed to image pairs I^L, \tilde{I}^L and I^R, \tilde{I}^R . At this point, since all the inputs are pseudo-stereo inputs, the network naturally cannot differentiate them further. As shown by the experiments in Section IV-B, the network achieves stable convergence to high performance and avoids overfitting under this strategy. At this point, (1) becomes,

$$L_p = \frac{1}{N} \sum_{ij} (p \cdot pe(I_{ij}^L, \tilde{I}_{ij}^L) + (1-p) \cdot pe(I_{ij}^R, \tilde{I}_{ij}^R)) \cdot \tilde{O}_{ij} \quad (3)$$

In addition to L_p , the same edge-aware smoothness L_s as in [12] is adopted, and the disparity values are also mean-normalized like them.

$$L_s = |\partial_x D^{L*}| e^{-|\partial_x I^L|} + |\partial_y D^{L*}| e^{-|\partial_y I^L|}, \quad (4)$$

where $D^{L*} = D^L / \overline{D^L}$. In our experiments, it is observed that an overly large smoothing loss at the early stages hinders the model’s exploration capability and has a slight negative impact on its final performance. Therefore, we modify the smoothing term to a parameter that gradually reaches the set value, reducing its influence in the early stages. The final loss can be expressed as:

$$L = L_p + \lambda L_s. \quad (5)$$

λ is the smoothing term coefficient, starting from 0.001 and gradually increasing to the set value of 0.5 over 10k iterations.

IV. EXPERIMENTS

In this section, we present experiments conducted with the methods proposed in this paper. Section IV-A compares our approach with existing supervised methods, data generation-based self-supervised methods and direct self-supervised

methods. The ablation study is conducted in Section IV-B to demonstrate the contributions of each component described previously.

Dataset. In order to contrast with prior research [6], [8], [11], [22], [26], our experiments utilize the same datasets: KITTI 2012 [27] and KITTI 2015 [28]. All training processes are conducted entirely using the self-supervised method without any ground truth, relying solely on image pairs as both inputs and feedback. Each dataset mentioned above consists of a training set and a testing set. The training set provides ground truth data, while results on the test set must be submitted to their website for evaluation. Given that self-supervised training only requires image pairs, we utilize all the image pairs in each dataset for training. The training set, which provides ground truth, is used for validation and ablation studies. Test set results are submitted to their website for evaluation and comparison with existing methods.

Training Details. We maintain consistent parameters across different datasets to demonstrate the robustness of our method. All training is conducted using a single RTX 4090 GPU in PyTorch [29]. We employ the Adam optimizer [30] with $\beta_1 = 0.9$, $\beta_2 = 0.999$ and the cosine annealing schedule. Following the settings in PSMNet [3], we crop images to 512×256 during training, with a batch size of 8. Data augmentation is applied to the input images but not to the feedback images. This augmentation consists of random cropping, brightness enhancement, and contrast adjustment. Convergence to optimal performance occurs after approximately $35k$ iterations, with a total training time of about 7 hours. The training process starts from scratch without any pre-training or post-processing involved.

A. Comparisons with State-of-the-art

In this section, our method is compared with other existing self-supervised methods [6], [8], [11], [13], [14], [17], [22], [26] and some representative supervised methods [2]–[4]. Given that all mentioned datasets offer clear online benchmarks, we first present the online benchmark results in Table I. The evaluation metrics are identical to those in the online

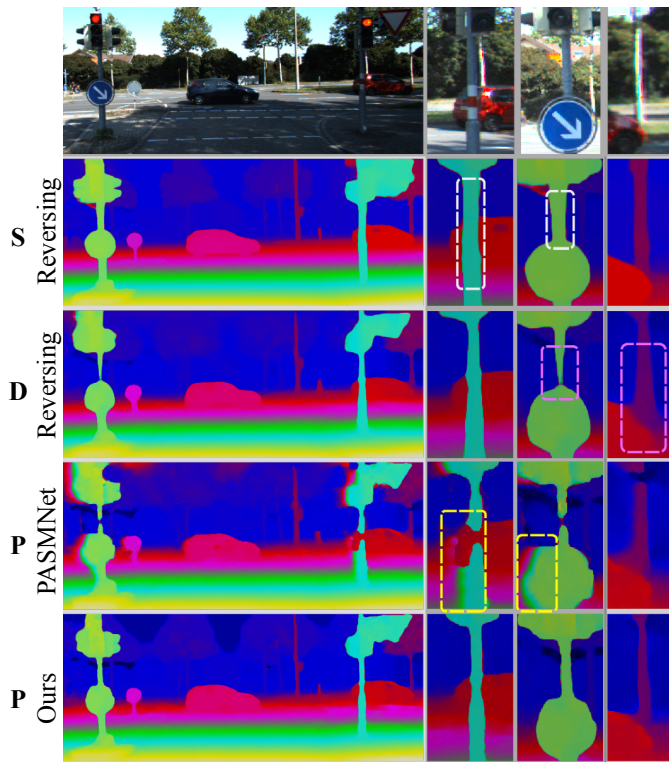


Fig. 6. Qualitative comparisons. Representative methods from different categories are selected, with all disparity maps sourced from the KITTI 2015 online benchmark. (S: supervised method; D: dataset generation-based method; P: direct self-supervised method based on photometric loss.)

benchmarks. Specifically, “noc” and “all” denote non-occluded pixels and all pixels respectively. “n-noc/all” refers to the percentage of pixels exceeding a difference of “n” from ground truth. “D1” indicates the proportion of pixels where the endpoint error is less than 3px or 5%. “EPE” represents the average difference between estimated values and ground truth. Since some methods lack online test results, we include their reported training set results from the paper for reference only. Generally, these metrics tend to perform worse on the test set compared to the training set.

The results in Table I demonstrate that our method significantly outperforms other direct self-supervised methods across the board. When compared to dataset generation-based methods, we only slightly lag behind Rversing-PSMNet [13], which integrates complex operations such as traditional methods, deep completion networks, and label distillation. In addition, it is shown that our results have partially outperformed the earlier representative supervised method DispNetC [2].

In Figure 6, we select representative methods from different categories for qualitative comparison with our approach. Specifically, this includes the representative of supervised methods (S), Los [4]; the representative of dataset generation-based methods (D), Reversing [13]; and the representative of direct self-supervised learning methods based on photometric loss (P), PASMNet [8]. Among these methods, PASMNet, which belongs to the same category as ours, is notably impacted by occlusion problems and generates extensive erroneous predictions. In contrast, our method maintains accurate

predictions in the same occluded regions. This suggests that the long-standing occlusion problem, which has been a hindrance in such methods, is addressed in our approach.

Further comparisons with the other two methods highlight our significant competitiveness even when compared to them. Furthermore, detailed comparisons reveal additional advantages of our method. Specifically, different training methods lead to distinct limitations and biases in their outputs. In Figure 6, rectangular boxes highlight the locations where errors occur in the comparative methods. Within the white boxes, it is shown that the supervised approach [4], heavily dependent on label data, outputs significantly broader edges because of erroneous ground truth. In the purple boxes, it is demonstrated that [13] exhibits excessive smoothing in ambiguous regions due to its reliance on labels generated by a monocular network. In contrast, our method does not rely on label data or data from other pre-processing methods. The direct self-supervised training based solely on images enables it to produce results closer to reality in the predicted disparity map. To further demonstrate this phenomenon, we select a typical scenario with problematic ground truth in Figure 1. In this scenario, supervised learning converges to incorrect results by strictly following the guidance of the ground truth. The previous self-supervised method fails to produce accurate results due to occlusion issues. Conversely, our self-supervised approach is unaffected by labeled data and also resolves occlusion problems, yielding more realistic predictions. This undoubtedly highlights the additional potential of our direct self-supervised method. Inadequately, as shown in Figure 1 (B) and (C), areas with highly indistinct colors and interference remain challenging for self-supervised approaches that rely on photometric consistency. The solution to this challenge could be crucial for advancing the framework introduced in this work.

B. Ablation Study

In this section, the roles of the various components proposed in Section III within the overall framework are studied and discussed. The components involved include the pseudo-stereo inputs strategy, the more accurate pseudo-image generation method, the occlusion estimation, and the fully pseudo-stereo inputs strategy. The experimental results under different combinations of components are shown in Table II. In this context, “PS” denotes the use of the pseudo-stereo inputs strategy, “Wider” indicates wider input for more accurate image generation, “Occ” represents occlusion estimation, and “FPS” signifies the adoption of the fully pseudo-stereo inputs strategy.

In the base method (a), common photometric loss is used, while other components such as smoothness loss, data augmentation methods, and training parameters are identical to those in the complete method. Obviously, the complete method (h) shows a significant improvement compared to the base method (a), in which none of the proposed strategies are applied. The contrast between (a) and (c) shows that merely implementing the pseudo-stereo inputs strategy leads to a substantial improvement in the base method. The comparisons between (c) and (e), as well as between (d) and (f), demonstrate that the introduction of occlusion estimation is crucial

TABLE II
ABLATION STUDY OF COMPONENTS IN THE PROPOSED METHOD.

	Method	PS	Wider	Occ	FPS	D1-all (%)	EPE-all	Remarks
(a)	base					5.67	1.17	
(b)	base + occ			✓		5.73	1.24	Over-smoothing in occlusion areas
(c)	Only pseudo-stere	✓				4.99	1.07	Overfitting
(d)	PS + fully pseudo strategy	✓			✓	5.17	1.11	/
(e)	PS + Occlusion detection	✓		✓		4.08	0.99	Overfitting
(f)	Only no wider generation	✓		✓	✓	4.31	1.04	/
(g)	Only no fully pseudo	✓	✓	✓		4.11	0.99	Slight overfitting
(h)	Pseudo-Stereo (full)	✓	✓	✓	✓	4.06	1.01	/

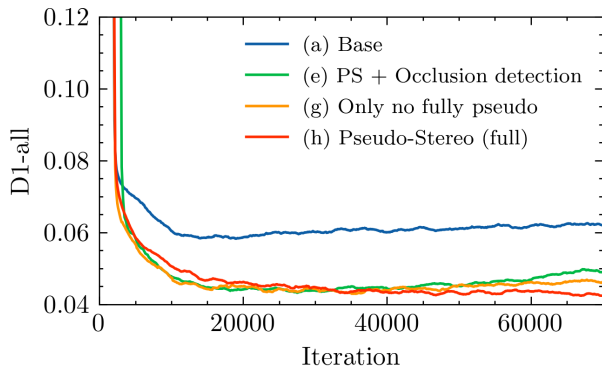


Fig. 7. Illustration of overfitting problems. Following the implementation of the fully pseudo-stereo inputs strategy (h), the upward trend of D1-all is no longer observed.

for performance improvement, regardless of whether the fully pseudo-stereo inputs strategy is adopted. The results from (c), (e), and (g) collectively indicate that overfitting is difficult to address without the fully pseudo-stereo inputs strategy. It is noteworthy that the comparison between (e) and (g) indicates more realistic and indistinguishable generated images can alleviate overfitting problems. In Figure 7, we plot the training process curves to visually illustrate this phenomenon. It is evident that the overfitting problem disappears when adopting the fully pseudo-stereo inputs strategy in (h). Finally, by comparing (e), (f), and (h), it can be inferred that using the fully pseudo-stereo inputs strategy will reduce accuracy to some extent when generated images exhibit noticeable defects. Conversely, when using a wider generation to produce more accurate images, this issue is effectively resolved. In general, within the overall framework, each component plays a distinct role. Through the combination of all components, we obtained highly accurate and stable training outcomes.

V. CONCLUSION

In this work, we propose a self-supervised stereo matching paradigm with the core idea of a pseudo-stereo inputs strategy. This method effectively addresses the occlusion issue, which has consistently hindered the performance of direct self-supervised stereo matching. Both qualitative and quantitative experiments demonstrate a significant improvement over existing direct self-supervised methods based on photometric consistency.

In future research, we aim to extend this methodology to other related challenges. For instance, similar occlusion issues

are also present in self-supervised optical flow estimation problems. The notable effectiveness of decoupling input and feedback images in stereo matching suggests a potential solution for addressing occlusions in self-supervised optical flow estimation as well. In addition to this, large visual models have now become crucial for further enhancing the capabilities of learning-based methods. Their reliance on vast amounts of training data has made the effective utilization of easily accessible unannotated data an urgent requirement. The self-supervised method proposed in this paper offers new insights into exploiting information from unlabeled stereo image pairs, which may be referenced for further application in these areas.

REFERENCES

- [1] M. Poggi, F. Tosi, K. Batsos, P. Mordohai, and S. Mattoccia, "On the Synergies between Machine Learning and Binocular Stereo for Depth Estimation from Images: A Survey," *IEEE Transactions on Pattern Analysis and Machine Intelligence*, pp. 1–1, 2021.
- [2] N. Mayer, E. Ilg, P. Hausser, P. Fischer, D. Cremers, A. Dosovitskiy, and T. Brox, "A Large Dataset to Train Convolutional Networks for Disparity, Optical Flow, and Scene Flow Estimation," in *2016 IEEE Conference on Computer Vision and Pattern Recognition (CVPR)*, (Las Vegas, NV, USA), pp. 4040–4048, IEEE, June 2016.
- [3] J.-R. Chang and Y.-S. Chen, "Pyramid stereo matching network," in *Proceedings of the IEEE Conference on Computer Vision and Pattern Recognition*, pp. 5410–5418, 2018.
- [4] K. Li, L. Wang, Y. Zhang, K. Xue, S. Zhou, and Y. Guo, "LoS: Local structure-guided stereo matching," in *Proceedings of the IEEE/CVF Conference on Computer Vision and Pattern Recognition*, pp. 19746–19756, 2024.
- [5] C. Zhou, H. Zhang, X. Shen, and J. Jia, "Unsupervised Learning of Stereo Matching," in *2017 IEEE International Conference on Computer Vision (ICCV)*, (Venice), pp. 1576–1584, IEEE, Oct. 2017.
- [6] A. Li and Z. Yuan, "Occlusion aware stereo matching via cooperative unsupervised learning," in *Asian Conference on Computer Vision*, pp. 197–213, Springer, 2018.
- [7] Y. Wang, P. Wang, Z. Yang, C. Luo, Y. Yang, and W. Xu, "UnOS: Unified Unsupervised Optical-Flow and Stereo-Depth Estimation by Watching Videos," in *2019 IEEE/CVF Conference on Computer Vision and Pattern Recognition (CVPR)*, (Long Beach, CA, USA), pp. 8063–8073, IEEE, June 2019.
- [8] L. Wang, Y. Guo, Y. Wang, Z. Liang, Z. Lin, J. Yang, and W. An, "Parallax attention for unsupervised stereo correspondence learning," *IEEE transactions on pattern analysis and machine intelligence*, vol. 44, no. 4, pp. 2108–2125, 2020.
- [9] R. Jonschkowski, A. Stone, J. T. Barron, A. Gordon, K. Konolige, and A. Angelova, "What matters in unsupervised optical flow," in *Computer Vision—ECCV 2020: 16th European Conference, Glasgow, UK, August 23–28, 2020, Proceedings, Part II 16*, pp. 557–572, Springer, 2020.
- [10] J. Hur and S. Roth, "Self-Supervised Multi-Frame Monocular Scene Flow," in *2021 IEEE/CVF Conference on Computer Vision and Pattern Recognition (CVPR)*, (Nashville, TN, USA), pp. 2683–2693, IEEE, June 2021.
- [11] R. Yang, X. Li, R. Cong, and J. Du, "Unsupervised Hierarchical Iterative Tile Refinement Network With 3D Planar Segmentation Loss," *IEEE Robotics and Automation Letters*, vol. 9, pp. 2678–2685, Mar. 2024.

- [12] C. Godard, O. M. Aodha, M. Firman, and G. Brostow, "Digging Into Self-Supervised Monocular Depth Estimation," in *2019 IEEE/CVF International Conference on Computer Vision (ICCV)*, (Seoul, Korea (South)), pp. 3827–3837, IEEE, Oct. 2019.
- [13] F. Aleotti, F. Tosi, L. Zhang, M. Poggi, and S. Mattoccia, "Reversing the cycle: Self-supervised deep stereo through enhanced monocular distillation," in *16th European Conference on Computer Vision (ECCV)*, Springer, 2020.
- [14] J. Watson, O. M. Aodha, D. Turmukhambetov, G. J. Brostow, and M. Firman, "Learning Stereo from Single Images," in *Computer Vision – ECCV 2020* (A. Vedaldi, H. Bischof, T. Brox, and J.-M. Frahm, eds.), vol. 12346, pp. 722–740, Cham: Springer International Publishing, 2020.
- [15] M. S. Hamid, N. Abd Manap, R. A. Hamzah, and A. F. Kadmin, "Stereo matching algorithm based on deep learning: A survey," *Journal of King Saud University-Computer and Information Sciences*, vol. 34, pp. 1663–1673, May 2022.
- [16] J. Zeng, C. Yao, Y. Wu, and Y. Jia, "Temporally consistent stereo matching," *European conference on computer vision (ECCV)*, 2024.
- [17] F. Tosi, A. Tonioni, D. De Gregorio, and M. Poggi, "NeRF-Supervised Deep Stereo," in *2023 IEEE/CVF Conference on Computer Vision and Pattern Recognition (CVPR)*, (Vancouver, BC, Canada), pp. 855–866, IEEE, June 2023.
- [18] I. Fang, H.-C. Wen, C.-L. Hsu, P.-C. Jen, P.-Y. Chen, Y.-S. Chen, et al., "ES3Net: Accurate and efficient edge-based self-supervised stereo matching network," in *Proceedings of the IEEE/CVF Conference on Computer Vision and Pattern Recognition*, pp. 4472–4481, 2023.
- [19] C. Godard, O. M. Aodha, and G. J. Brostow, "Unsupervised Monocular Depth Estimation with Left-Right Consistency," in *2017 IEEE Conference on Computer Vision and Pattern Recognition (CVPR)*, (Honolulu, HI), pp. 6602–6611, IEEE, July 2017.
- [20] C. Wang, J. M. Buenaposada, R. Zhu, and S. Lucey, "Learning Depth from Monocular Videos Using Direct Methods," in *2018 IEEE/CVF Conference on Computer Vision and Pattern Recognition*, (Salt Lake City, UT, USA), pp. 2022–2030, IEEE, June 2018.
- [21] J. Watson, M. Firman, G. Brostow, and D. Turmukhambetov, "Self-Supervised Monocular Depth Hints," in *2019 IEEE/CVF International Conference on Computer Vision (ICCV)*, (Seoul, Korea (South)), pp. 2162–2171, IEEE, Oct. 2019.
- [22] P. Liu, I. King, M. R. Lyu, and J. Xu, "Flow2Stereo: Effective Self-Supervised Learning of Optical Flow and Stereo Matching," in *2020 IEEE/CVF Conference on Computer Vision and Pattern Recognition (CVPR)*, pp. 6647–6656, June 2020.
- [23] V. Tankovich, C. Hane, Y. Zhang, A. Kowdle, S. Fanello, and S. Bouaziz, "HITNet: Hierarchical Iterative Tile Refinement Network for Real-time Stereo Matching," in *2021 IEEE/CVF Conference on Computer Vision and Pattern Recognition, Cvpr 2021*, pp. 14357–14367, 2021.
- [24] H. Hirschmuller, "Accurate and efficient stereo processing by semi-global matching and mutual information," in *2005 IEEE Computer Society Conference on Computer Vision and Pattern Recognition (CVPR '05)*, vol. 2, pp. 807–814 vol. 2, June 2005.
- [25] Y. Wang, Y. Yang, Z. Yang, L. Zhao, P. Wang, and W. Xu, "Occlusion Aware Unsupervised Learning of Optical Flow," in *2018 IEEE/CVF Conference on Computer Vision and Pattern Recognition*, (Salt Lake City, UT), pp. 4884–4893, IEEE, June 2018.
- [26] X. Fan, S. Jeon, and B. Fidan, "Occlusion-Aware Self-Supervised Stereo Matching with Confidence Guided Raw Disparity Fusion," in *2022 19th Conference on Robots and Vision (CRV)*, pp. 132–139, May 2022.
- [27] A. Geiger, P. Lenz, and R. Urtasun, "Are we ready for autonomous driving? The KITTI vision benchmark suite," in *2012 IEEE Conference on Computer Vision and Pattern Recognition*, (Providence, RI), pp. 3354–3361, IEEE, June 2012.
- [28] M. Menze and A. Geiger, "Object Scene Flow for Autonomous Vehicles," in *Proceedings of the IEEE Conference on Computer Vision and Pattern Recognition*, pp. 3061–3070, 2015.
- [29] A. Paszke, S. Gross, F. Massa, A. Lerer, J. Bradbury, G. Chanan, T. Killeen, Z. Lin, N. Gimelshein, L. Antiga, et al., "Pytorch: An imperative style, high-performance deep learning library," *Advances in neural information processing systems*, vol. 32, 2019.
- [30] D. P. Kingma and J. Ba, "Adam: A method for stochastic optimization.," in *The Eleventh International Conference on Learning Representations* (Y. Bengio and Y. LeCun, eds.), 2015.